View metadata, citation and similar papers at core.ac.uk

brought to you by CORE

provided by Florence Research

Ergodicity in randomly perturbed quantum systems

This content has been downloaded from IOPscience. Please scroll down to see the full text.

2017 Quantum Sci. Technol. 2 015007

(http://iopscience.iop.org/2058-9565/2/1/015007)

View the table of contents for this issue, or go to the journal homepage for more

Download details:

IP Address: 150.217.156.142
This content was downloaded on 17/03/2017 at 17:33

Please note that terms and conditions apply.

You may also be interested in:

Stochastic quantum zeno by large deviation theory
Stefano Gherardini, Shamik Gupta, Francesco Saverio Cataliotti et al.

Discrete dynamics and non-Markovianity
Kimmo Luoma and Jyrki Piilo

Strongly interacting ultracold polar molecules
Bryce Gadway and Bo Yan

Quantum state reconstruction on atom–chips
C Lovecchio, S Cherukattil, B Cilenti et al.

Observation of quantum Zeno effect in a superconducting flux qubit
K Kakuyanagi, T Baba, Y Matsuzaki et al.

Loschmidt echo in many-spin systems: a quest for intrinsic decoherence and emergent irreversibility
Pablo R Zangara and Horacio M Pastawski

Activated and non-activated dephasing in a spin bath
E Torrontegui and R Kosloff

Scanning electron microscopy of cold gases
Bodhaditya Santra and Herwig Ott

Zeno--anti-Zeno crossover dynamics in a spin--boson system
A Thilagam

Quantum Science and Technology

RECEIVED
12 August 2016

REVISED
15 December 2016

ACCEPTED FOR PUBLICATION
30 January 2017

PUBLISHED
7 March 2017

PAPER

Ergodicity in randomly perturbed quantum systems

Stefano Gherardini[1,2], Cosimo Lovecchio[1], Matthias M Müller[1], Pietro Lombardi[1,3], Filippo Caruso[1,3,4] and Francesco Saverio Cataliotti[1,3]

[1] LENS, QSTAR, and Department of Physics and Astronomy, University of Florence, via G. Sansone 1, I-50019 Sesto Fiorentino, Italy
[2] INFN, CSDC and Department of Information Engineering, University of Florence, via S. Marta 3, I-50139 Florence, Italy
[3] INO-CNR,UOS Sesto Fiorentino, via N. Carrara 1, I-50019 Sesto Fiorentino, Italy
[4] Author to whom any correspondence should be addressed.

E-mail: filippo.caruso@lens.unifi.it

Keywords: quantum Zeno phenomena, ergodicity, atom chips, stochastic quantum measurements

Abstract

The theoretical cornerstone of statistical mechanics is the ergodic assumption, i.e. the assumption that the time average of an observable equals its ensemble average. Here, we show how such a property is present when an open quantum system is continuously perturbed by an external environment effectively *observing* the system at random times while the system dynamics approaches the quantum Zeno regime. In this context, by large deviation theory we analytically show how the most probable value of the probability for the system to be in a given state eventually deviates from the non-stochastic case when the Zeno condition is not satisfied. We experimentally test our results with ultra-cold atoms prepared on an atom chip.

1. Introduction

Ergodicity plays a key role in statistical physics. In classical mechanics it was introduced by Boltzmann [1] and corresponds to the fact that over a long period of time all portions of phase space (of constant energy) are visited for a time proportional to the respective phase space volume. As a consequence, time and ensemble (i.e. phase space) average of dynamical variables coincide each other for an ergodic system. Then, the notion of ergodicity was first extended to quantum mechanics by von Neumann [2, 3]. The main difficulties were the quantum generalisation of the classical phase space, as investigated later by Wigner [4], and the concept of distance between quantum states. The von Neumann definition of ergodicity has then been criticised as summarised in [5–7]. This has led to a revised definition of quantum ergodicity by Peres [5] based on his definition of quantum chaos, and by considering observables as time dependent operators in the Heisenberg picture. He has hence defined quantum ergodicity by the equality of the time average of an arbitrary quantum operator and its ensemble average. More recently, in [7, 8] quantum ergodicity has been studied in terms of the energy structure of the system, namely its eigenenergies and energy spacings. The absence of degeneracies then leads to the ergodic property of coinciding time and ensemble averages, without involving the notion of quantum chaos. Moreover, ergodic dynamics has been demonstrated in a small quantum system consisting of only three superconducting qubits, as a platform for investigating various phenomena in non-equilibrium thermodynamics [9].

In a different framework, the theory of large deviations (LD) allows one to investigate the asymptotic exponential decay of probabilities associated with large fluctuations of stochastic variables, for both classical and quantum systems [11–13]. The LD theory has been discussed in the context of quantum gases [14], quantum spin systems [15] and, especially, quantum jump trajectories [16, 17] for open quantum systems. In the latter case, the thermodynamics of a quantum system in continuous interaction with the environment (external reservoir) has been studied and the statistics of quantum jumps in the long time limit has been treated from the point of view of dynamical phase transitions in the trajectory space. As a matter of fact, the dynamics of any open quantum system can be always described in terms of a unitary interaction between the system and an external environment followed by a projective (jump) measurement [18].

An open system, i.e. a system exchanging energy and/or matter with its external environment (usually far from an equilibrium regime), is dissipative when its total energy is not a preserved quantity, and the system

© 2017 IOP Publishing Ltd

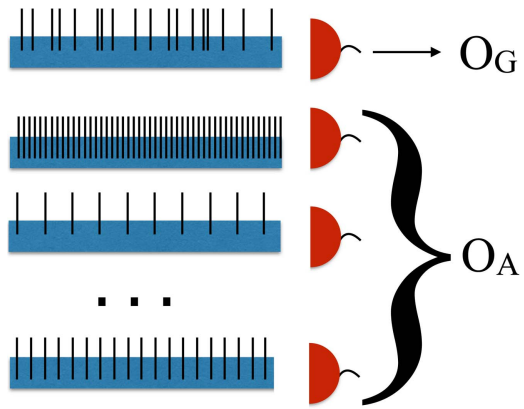

Figure 1. Pictorial representation of two measurement schemes on an open quantum system, corresponding, respectively, to here called geometric O_G and arithmetic O_A averages of a generic observable O. The black lines represent the interaction with the external environment that is mimicked by consecutive projective measurements on the system. Note that the total time, corresponding to a given realisation of the measurement sequence, is a random variable depending on how the stochasticity is realised.

integrability turns out to be broken [10]. In our case, the dissipation is introduced by applying stochastic quantum measurements to a finite-dimensional quantum system realised with cold atoms, and we study the survival probability of the quantum system in its initial state. The fluctuations in the measurement outcomes both in time and for different realisations allow us to define an equivalent of time and ensemble averages, and to study an ergodic property of the system.

It is worth emphasising how the monitoring of a given quantum system by a frequent enough series of measurements is linked to the well-known quantum Zeno effect (QZE) [19, 20], resulting from the statistical indistinguishability of neighbouring quantum states [21]. Experimentally, the quantum Zeno effect has been observed on a wide range of different experimental platforms, with ions [22], polarised photons [23], and cold atoms [24]. In particular, in [24] in a system of cold sodium atoms trapped in a far-detuned standing wave of light, it has been observed how the decay features of the atoms are suppressed (Zeno effect) or enhanced (anti-Zeno effect) with respect to the unperturbed case, according to the frequency of the measurements. Very recently, the stochastic quantum Zeno effect (SQZE) has been introduced [25, 26], analysing the dependence of Zeno phenomena on a source of randomness in a protective measurement sequence. In particular, in [26] a general quantum system subjected to an arbitrary but fixed number of consecutive projective measurements is considered. If the time interval between the measurements is randomly distributed, the survival probability, i.e. the probability to remain in the initial quantum state is itself a random variable taking on different values corresponding to different realisations of the measurement sequence. The sensitivity of such survival probability with respect to the stochasticity in the time interval between the measurements has been also quantified by means of the Fisher information [27].

The main result of the present article is the theoretical and experimental demonstration, by applying LD theory, of the equivalence between the analogous of time and ensemble averages of the corresponding stochastic series of quantum projective measurements, hence the presence of ergodicity, when approaching the quantum Zeno regime. This property will pave the way towards the development of new feasible schemes to control quantum systems by tunable and usually deleterious stochastic noise.

Given an observable O, we introduce two schemes to take into account the presence of stochastic noise arising from an external environment applying effectively consecutive quantum projective measurements to the system, as shown in figure 1. The first scheme is based on the measurement of O after the single dynamical evolution of a system that does interact with the environment at times being stochastically distributed (geometric average O_G). The second scheme consists of the averaging of the final observable outcomes over different dynamical realisations of the system each periodically interacting with the environment (arithmetic average O_A). Then, different realisations correspond to different time intervals in the system-environment interaction, but extracted from the same stochastic probability distribution as in the first scheme. The total number of times in which the time interval is sampled by the probability distribution, moreover, establishes the relative weight to compute the arithmetic average O_A. The reason why they are, respectively, called geometric and arithmetic averages will be clearer in the following, as well as their relation to the time and ensemble averages. We realised these schemes experimentally using a Bose–Einstein condensate (BEC) of Rubidium (^{87}Rb) atoms, prepared on an atom chip [28].

2. Methods

2.1. Theory

Let us consider a quantum mechanical system under the evolution of a time-independent Hamiltonian H and initially prepared in a state $\rho_0 = |\psi_0\rangle\langle\psi_0|$. Then, it is subjected to m consecutive projective measurements with projection operator $P = |\psi_0\rangle\langle\psi_0|$ after intervals of free evolution of time length μ_j $(j = 1, \ldots, m)$. The observable O is represented by the projection operator onto the state $|\psi_0\rangle$, i.e. $O = P$. The quantum mechanical expectation value of O here corresponds to the so-called survival probability, namely, the probability that the system is still in the initial state at the end of the evolution. We take the μ_j to be independent and identically distributed (i.i.d.) random variables sampled from a given distribution $p(\mu)$, with the normalisation $\int d\mu\ p(\mu) = 1$ and the mean value $\overline{\mu}$. The density matrix at the end of the evolution for a total time $\mathcal{T} \equiv \sum_{j=1}^{m} \mu_j$, corresponding to a given realisation of the measurement sequence $\{\mu_j\} \equiv \{\mu_j;\ j = 1, 2, \ldots, m\}$, is given by

$$\rho(\{\mu_j\}) = \frac{R_m(\{\mu_j\})\rho_0 R_m^{\dagger}(\{\mu_j\})}{\mathcal{P}(\{\mu_j\})}, \tag{1}$$

where we have defined $R_m(\{\mu_j\}) \equiv \prod_{j=1}^{m} PU_jP$, with $U_j \equiv \exp(-iH\mu_j)$, and

$$\mathcal{P}(\{\mu_j\}) = \mathrm{Tr}\left[R_m(\{\mu_j\})\rho_0 R_m^{\dagger}(\{\mu_j\})\right] \tag{2}$$

is the survival probability. The reduced Planck's constant $\hbar$ is set to unity. Note that $\mathcal{T}$ is a random variable that depends on the realisation of the sequence $\{\mu_j\}$, while $\mathcal{P}(\{\mu_j\})$ depends on the system Hamiltonian H [29], the initial density matrix ρ_0, and also on the probability distribution $p(\mu)$.

The survival probability can be also expressed as

$$\mathcal{P}(\{\mu_j\}) = \prod_{j=1}^{m} q(\mu_j), \tag{3}$$

where $q(\mu_j) \equiv |\langle\psi_0|U_j|\psi_0\rangle|^2$ is the survival probability after a single measurement. In this way, by using LD theory, one can derive the probability distribution of the survival probability $\mathcal{P}(\{\mu_j\})$, $\mathrm{Prob}(\mathcal{P})$, with respect to different realisations of the sequence $\{\mu_j\}$ [12, 26]. According to the shape of $p(\mu)$, one can calculate the survival probability's ensemble average, i.e.

$$\langle\mathcal{P}(m)\rangle \equiv \left(\int_{\mu} d\mu p(\mu) q(\mu)\right)^m = \exp\left(m \ln \int_{\mu} d\mu p(\mu) q(\mu)\right), \tag{4}$$

and its most probable value, defined as the value which minimises the rate function $J(\mathcal{P}) \equiv \lim_{m\to\infty}\{-\ln[\mathrm{Prob}(\mathcal{P})]/m\}$. In [26], it has been proved that this most probable value is equivalent to the log-average of the quantity $q(\mu)$ with respect to $p(\mu)$, namely to the geometric average $\overline{\mathcal{P}}_g$ of the survival probability weighted by $p(\mu)$:

$$\overline{\mathcal{P}}_g \equiv \prod_{\{\mu\}} q(\mu)^{mp(\mu)} = \exp\left(\int_{\mu} d\mu p(\mu) \ln(q(\mu)^m)\right), \tag{5}$$

where index of multiplication assumes all possible values $\{\mu\}$, i.e. the ones in the support of $p(\mu)$. In the limit of a large number of measurements M, the geometric average $\overline{\mathcal{P}}_g(m)$ is the value to which the time average

$$\hat{\mathcal{P}}_M(m) \equiv \frac{1}{M}\sum_{k=1}^{M} \mathcal{P}(\{\mu_j\}_{j=1}^{k})^{\frac{m}{k}} \tag{6}$$

of the survival probability $\mathcal{P}(\{\mu_j\})$ converges:

$$\hat{\mathcal{P}}(m) \equiv \lim_{M\to\infty} \frac{1}{M}\sum_{k=1}^{M} \mathcal{P}(\{\mu_j\}_{j=1}^{k})^{\frac{m}{k}} = \overline{\mathcal{P}}_g(m). \tag{7}$$

Note that the survival probability's value after m measurements can be estimated by using the corresponding value $\mathcal{P}(\{\mu_j\}_{j=1}^{k})$ after k measurements, by the relation $\mathcal{P}(\{\mu_j\}_{j=1}^{m}) \approx \mathcal{P}(\{\mu_j\}_{j=1}^{k})^{\frac{m}{k}}$. This value, then, is averaged for $k = 1, \ldots, M$, and in the limit of large M converges to the geometric average.

Additionally, one can consider the ordered case of periodic projective measurements, i.e. $\mu_j = \mu$, but with μ being selected according to $p(\mu)$. This leads to the definition of the arithmetic average, i.e.

$$\overline{\mathcal{P}}_a \equiv \int_{\mu} d\mu p(\mu) q(\mu)^m = \exp\left(\ln \int_{\mu} d\mu p(\mu) q(\mu)^m\right). \tag{8}$$

Using Jensen's inequality, namely $\langle\ln(x)\rangle \leqslant \ln(\langle x\rangle)$, and considering that $\langle x\rangle^m \leqslant \langle x^m\rangle$ for any $x \in [0, 1]$ and $m \in \mathbb{N}$, it follows that $\overline{\mathcal{P}}_g \leqslant \langle\mathcal{P}\rangle \leqslant \overline{\mathcal{P}}_a$.

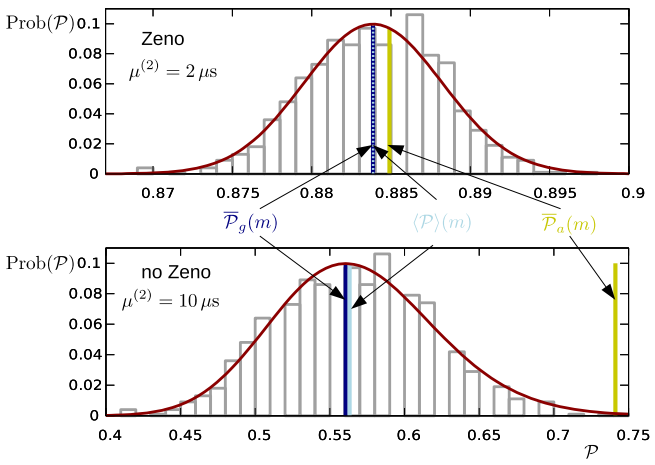

Figure 2. Probability distribution Prob $(\mathcal{P})$ of the survival probability. The grey boxes refers to the relative frequencies of $\mathcal{P}$, obtained by evaluating numerically 1000 random realisations of the survival probability after $m = 100$ measurements. They are compared to the expected distribution shown in dark red, equation (13). The top panel shows the results in the Zeno regime, the lower panel for violated Zeno condition. As it can be seen, the values of the geometric average $\overline{\mathcal{P}}_g$ and of the expectation value $\langle\mathcal{P}\rangle$ are very similar. In the Zeno limit, also $\overline{\mathcal{P}}_a$ is very close to these two values, unlike the lower panel where the Zeno condition does not hold, hence demonstrating the ergodic hypothesis for a randomly perturbed quantum system only in the Zeno regime.

As stated, the main result of this Letter is the theoretical demonstration and the experimental observation that in the *Zeno regime* it is sufficient to examine the series of constant μ in order to determine $\overline{\mathcal{P}}_g$, $\overline{\mathcal{P}}_a$ and $\langle\mathcal{P}\rangle$. This *Zeno regime* is defined by

$$m\int p(\mu)\ln q(\mu)\,d\mu = m\,\langle\ln q(\mu)\rangle \ll 1. \tag{9}$$

Within this limit, indeed, all three averages are equal:

$$\overline{\mathcal{P}}_a \approx \langle 1 + m\ln q\rangle = 1 + m\,\langle\ln q\rangle \approx \overline{\mathcal{P}}_g, \tag{10}$$

and as a consequence of the relation $\overline{\mathcal{P}}_g \leqslant \langle\mathcal{P}\rangle \leqslant \overline{\mathcal{P}}_a$, the equality holds also for the value of the ensemble average. Since in the geometric average the noise is averaged in time, while the other two averages are averages over different realisations, this equality means that the system dynamics is ergodic. More specifically, we can define the normalised discrepancy D between $\overline{\mathcal{P}}_g$ and $\overline{\mathcal{P}}_a$ as

$$D \equiv \frac{\overline{\mathcal{P}}_a - \overline{\mathcal{P}}_g}{\overline{\mathcal{P}}_a} = 1 - e^{-\Delta q(\mu,m)} \approx \Delta q(\mu,\, m), \tag{11}$$

where $\Delta q(\mu,\, m) \equiv \ln\langle q(\mu)^m\rangle - \langle\ln q(\mu)^m\rangle$. Note that $\Delta q(\mu,\, m)$ is approximately equal to zero in the Zeno regime, otherwise the equality in equation (10) (second-order Zeno approximation) breaks down. Indeed, the leading term in D is of fourth order in μ, i.e.

$$\Delta q(\mu,\, m) \approx \frac{m^2}{2}(\Delta^2 H)^2(\nu_4 - \nu_2^2), \tag{12}$$

which is determined by the second and the fourth moment of $p(\mu)$ ($\nu_2 = \int_\mu d\mu\; p(\mu)\mu^2$ and $\nu_4 = \int_\mu d\mu\; p(\mu)\mu^4$, respectively) and by the variance of the energy $\Delta^2 H$, and scales quadratically with the number of measurements m (see appendix A).

For better clarity let us consider a bimodal distribution for $p(\mu)$, with values $\mu^{(1)}$ and $\mu^{(2)}$ and probability p_1 and $p_2 = 1 - p_1$. The survival probability in the Stirling approximation for m sufficiently large is distributed as

$$\text{Prob}(\mathcal{P}) \approx \frac{1}{\sqrt{2\pi m p_1 p_2}}\exp\left(-\frac{(k(\mathcal{P}) - mp_1)^2}{2\,mp_1p_2}\right), \tag{13}$$

$$k(\mathcal{P}) = \frac{\ln\mathcal{P} - m\ln q(\mu^{(2)})}{\ln q(\mu^{(1)}) - \ln q(\mu^{(2)})}, \tag{14}$$

where $k(\mathcal{P})$ is the frequency of the event $\mu^{(1)}$ (see appendix B). Figure 2 shows the distribution Prob $(\mathcal{P})$ of the survival probability for this bimodal distribution. The grey boxes show the relative frequencies of $\mathcal{P}$ with $\mu^{(1)} = 1\;\mu$s after $m = 100$ measurements for 1000 random realisations as compared to the expected distribution, equation (13) shown in dark red. The top panel shows the results for $\mu^{(2)} = 2\;\mu$s (satisfying Zeno condition and ergodic), the lower panel for $\mu^{(2)} = 10\;\mu$s (not satisfying Zeno condition and not ergodic). We select two values of $\mu^{(2)}$ (i.e., 2 μs and 10 μs) in order to show two different scenarios closely related to the experimental observations (see figure 5). Indeed,

Table 1. Arithmetic and geometric averages $\overline{\mathcal{P}}_a$ and $\overline{\mathcal{P}}_g$ as a function of the probability p_1 for a bimodal distribution $p(\mu)$, expressed with four decimal digits. In the simulations we have chosen $\mu^{(1)} = 1\ \mu$s, $\mu^{(2)} = 10\ \mu$s, $\Delta H = 2\pi \cdot 2.5$ kHz, and $m = 100$.

p_1	$\overline{\mathcal{P}}_a$	$\overline{\mathcal{P}}_g$
0.01	0.0905	0.0842
0.05	0.1234	0.0927
0.2	0.2470	0.1329
0.5	0.4941	0.2729
0.8	0.7412	0.5606
0.95	0.8648	0.8035
0.99	0.8977	0.8845

$\mu^{(2)} = 2\ \mu$s is close to the minimal time interval that is experimentally feasible and leads to Zeno dynamics in a regime where the geometric average $\overline{\mathcal{P}}_g$ can also be different from 1 (depending on the choice of p_2). On the other side, $\mu^{(2)} = 10\ \mu$s guarantees that the Zeno condition is violated with $\overline{\mathcal{P}}_g$ being however significantly larger than zero. In both scenarios $\overline{\mathcal{P}}_g$ is the maximal value of Prob$(\mathcal{P})$ and the expectation value $\langle\mathcal{P}\rangle$ is very close to it. In the Zeno limit, also $\overline{\mathcal{P}}_a$ is very close to these two values, while in the lower panel, where the Zeno condition is violated, it assumes a distinctly different value, confirming the analytical results. The other parameters are $\Delta H = 2\pi \cdot 2.5$ kHz, $p_1 = 0.8$ and $p_2 = 0.2$. Qualitatively similar behaviours have been observed for other parameter values. In table 1 we show the difference between the values of $\overline{\mathcal{P}}_a$ and $\overline{\mathcal{P}}_g$ for a bimodal distribution when varying the probability p_1 but with $\mu^{(2)} = 10\ \mu$s. Outside the Zeno regime, the arithmetic average $\overline{\mathcal{P}}_a$ is always different from the geometric average $\overline{\mathcal{P}}_g$. Such discrepancy disappears when the stochasticity in the time interval between the measurements vanishes, i.e. for $p_1 = 0$ (complete leakage) and for $p_1 = 1$ (standard Zeno regime). All the theoretical predictions are well corroborated by the experimental data.

2.2. Experimental methods

We experimentally test our model with a Bose–Einstein condensate of ^{87}Rb produced in a magnetic micro-trap realised with an atom chip. The trap has a longitudinal frequency of 46 Hz, the radial trapping frequency is 950 Hz. The atoms are evaporated to quantum degeneracy by ramping down the frequency of a radio frequency (RF) field. The BEC has typically $8{\cdot}10^4$ atoms, a critical temperature of 0.5 μK and is at 300 μm from the chip surface. The magnetic fields for the micro-trap are provided by a Z-shaped wire on the atom chip and an external pair of Helmholtz coils. The RF fields for evaporation and manipulation of the Zeeman states are produced by two further conductors also integrated on the atom chip.

We note that the ground state of ^{87}Rb is a hyperfine doublet separated by 6.834 GHz with total spin $F = 2$ and $F = 1$, respectively. To prepare the atoms for the experiment, the condensate is released from the magnetic trap and allowed to expand freely for 0.7 ms while a constant magnetic field bias of 6.179 G is applied in a fixed direction. This procedure ensures that the atom remain oriented in state $|F = 2,\ m_F = +2\rangle$ and strongly suppresses the effect of atom-atom interactions by reducing the atomic density. The preparation consists in three steps. In the first step all the atoms are brought into the $|F = 2,\ m_F = 0\rangle$ state (see figure 3) with high fidelity ($\sim$95%). This is obtained applying a 50μs long frequency modulated RF pulse designed with an optimal control strategy [31]. After the RF pulse we transfer the whole $|F = 2,\ m_F = 0\rangle$ population into the $|F = 1,\ m_F = 0\rangle$ sub-level by shining in bichromatic (Raman) laser light. This is the initial state ρ_0 for our experiment. Note, that with our choice of laser polarisations and thanks to the presence of the homogeneous bias field shifting away from resonance other magnetic sub-levels, the bichromatic light does not alter the population of any other magnetic sub-levels. The preparation is completed by applying another RF pulse to place some atomic population in the $|F = 2,\ m_F = \pm 1\rangle$ states for normalization of the imaging procedure. Atoms in these last states will be not affected during the actual experiment, so they can be used as a control sample population.

In order to check each step of the preparation procedure, we record the number of atoms in each of the 8 m_F-states by applying a Stern–Gerlach method. In this regard, an inhomogeneous magnetic field is applied along the quantisation axis for 10 ms. This causes the different m_F-sub-levels to spatially separate. After a total time of 23 ms of expansion we shine in a monochromatic light on resonance with the $|F = 2\rangle \rightarrow |F' = 3\rangle$ transition for 200 μs, pushing away all atoms in the $F = 2$ sub-levels and recording the shadow cast by these atoms onto a CCD camera. We let the remaining atoms expand for further 1 ms and then we apply a bichromatic pulse containing light resonant to the $|F = 2\rangle \rightarrow |F' = 3\rangle$ and $|F = 1\rangle \rightarrow |F' = 2\rangle$ transitions, effectively casting onto the CCD the shadow of the atoms in the $F = 1$ sub-levels. Another two CCD images to acquire the background complete the imaging procedure.

The experiments are performed by coupling the $|F = 1,\ m_F = 0\rangle$ and $|F = 2,\ m_F = 0\rangle$ with the same Raman transition used for preparation, driven at a Rabi frequency of 5 kHz by a bichromatic laser beam (figure 4). Since we are working with ground state atoms, with our choice of laser polarisations and thanks to the presence of the

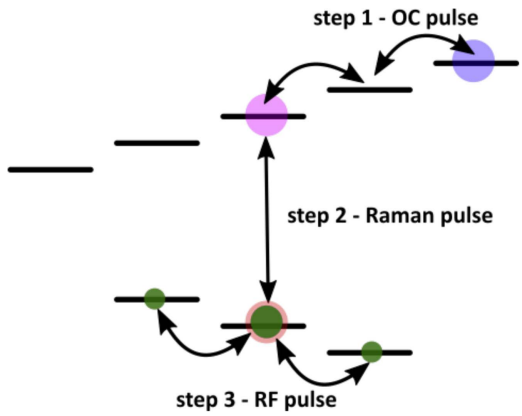

Figure 3. State preparation sequence for the SQZE experiment. After the condensation in the pure state $|F = 2,\ m_F = +2\rangle$, in the first step the atoms are transferred to the state $|F = 2,\ m_F = 0\rangle$ with fidelity ~95%. In the second step, by two Raman lasers the atoms in this sub-level are transferred to the lower state $|F = 1,\ m_F = 0\rangle$, which is the initial state ρ_0 for our experiment. In the third and last step, a fixed amount of population is transferred in the side sub-levels $|F = 1,\ m_F = \pm 1\rangle$. These atoms will be used as a benchmark to calculate the survival probability after the experiment.

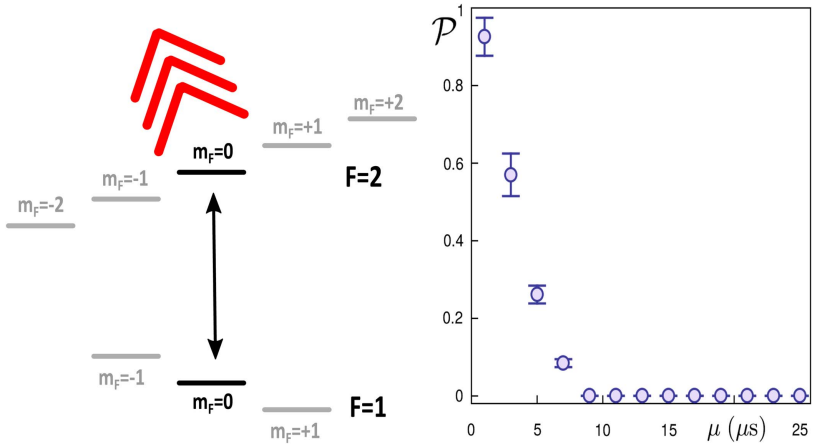

Figure 4. Confinement induced by pulsed quantum Zeno effect. The ground state structure of the ^{87}Rb in presence of a magnetic field consists of two hyperfine levels ($F = 1$ and $F = 2$), with no internal degeneracy. A laser induced Raman transition couples the sub-levels $|F = 1,\ m_F = 0\rangle$ and $|F = 2,\ m_F = 0\rangle$, while a laser on resonance with the transition $|F = 2\rangle \rightarrow |F' = 3\rangle$ (red arrows in the picture) depletes the population of the former. If the laser is strong enough, this equates to a projective measurement. On the right we show the typical exponential decay of the survival probability of the atoms in the $|F = 1,\ m_F = 0\rangle$ sub-level while the Raman coupling is on, and simultaneously the laser resonant to the $|F = 2\rangle \rightarrow |F' = 3\rangle$ transition is pulsed 100 times. The survival probability is plotted as a function of the interval μ between two pulses.

homogeneous bias field shifting away from resonance other magnetic sub-levels and selection rules for Raman transitions, we have effectively isolated a closed 2-level system. We realise the projective measurements $P = |\psi_0\rangle\langle\psi_0|$ by shining the atoms with a 1 μs pulse of imaging light, resonant with the $|F = 2\rangle \rightarrow |F' = 3\rangle$ component of the Rubidium $D2$ line. Note that from the excited state $|F' = 3\rangle$ atoms will immediately decay outside the condensate and will not be seen by our imaging system. Under constant coupling by the Raman beams, we apply 100 projective measurement P after variable intervals of free evolution μ_j. At the end of the sequence we measure the population remaining in state $|F = 1,\ m_F = 0\rangle$ and normalise it by comparison with the population in states $|F = 1,\ m_F = \pm 1\rangle$. This allows to measure, in a single shot, the survival probability $\mathcal{P}$ of the atoms in the initial state. Each experimental sequence is repeated 7 times to obtain averages and standard deviations.

3. Results

To realise the theoretical predictions experimentally we measure the geometric and arithmetic averages of the survival probability for an underlying bimodal distribution, where we take $\mu^{(1)} = 2$ μs to be fixed and $\mu^{(2)}$ variable between 2 μs and 25 μs.

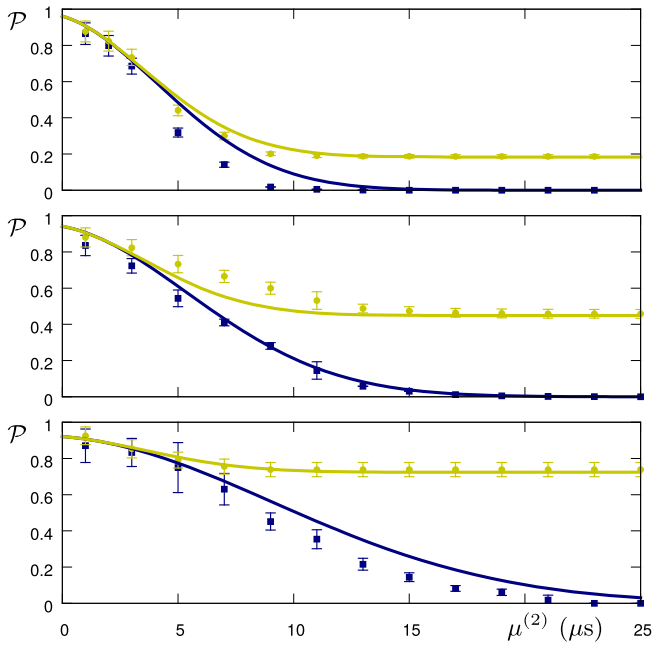

Figure 5. Scaling of $\overline{\mathcal{P}}_g$ (blue) and $\overline{\mathcal{P}}_a$ (yellow) with the interval length $\mu^{(2)}$ of a bimodal distribution for $p(\mu)$. In all three cases $\mu^{(1)} = 2\ \mu$s, $\Delta H = 2.5$ kHz. The probabilities of the bimodal distribution $(p_1,\ p_2)$ are $(0.2,\ 0.8)$ (upper panel), $(0.5,\ 0.5)$ (middle panel), and $(0.8,\ 0.2)$ (lower panel). The solid lines are theoretical curves, the single points are experimental values where the error bars indicate the standard deviation of the experimental error. The Zeno regime corresponds to vanishing μ_2.

In a first set of experiments we measure the arithmetic average $\overline{\mathcal{P}}_a$ by fixing the intervals of free evolution μ_j to be all the same and equal to $\mu \in \{\mu^{(1)},\ \mu^{(2)}\}$ and determine $\mathcal{P}(\mu)$, i.e the probability for an atom to remain in the initial state as a function of μ. As shown in figure 4, $\mathcal{P}(\mu)$ displays the characteristic exponential decay, becoming negligible, in our case, after 9 μs. After measuring $\mathcal{P}(\mu^{(1)})$ and $\mathcal{P}(\mu^{(2)})$, we then calculate the arithmetic average of the two data with statistical weights p_1 and p_2, respectively. In this way we obtain $\overline{\mathcal{P}}_a(\mu^{(2)})$ which represents the statistical mean averaged over the two possible system configurations as a function of the variable time $\mu^{(2)}$. In figure 5 we report as yellow dots the results of three choices $(0.2,\ 0.8)$, $(0.5,\ 0.5)$, and $(0.8,\ 0.2)$ for the statistical weights $(p_1,\ p_2)$.

In order to determine the geometric average $\overline{\mathcal{P}}_g$ of a single realisation, we perform a second set of experiments. In each experimental sequence we now choose the intervals of free evolution μ_j from a bimodal distribution given by $\mu^{(1)}$ and $\mu^{(2)}$ with probabilities $(p_1,\ p_2)$. The results of these experiments give the geometrical average $\overline{\mathcal{P}}_g(\mu^{(2)})$ of the survival probability as a function of the parameter $\mu^{(2)}$. We again choose the probabilities $(0.2,\ 0.8)$, $(0.5,\ 0.5)$, and $(0.8,\ 0.2)$ and report the experimental results, as blue squares in figure 5. As can be seen in the figure, the agreement of theoretical predictions and experiments is generally very good, although some deviations go beyond the error bars and are systematic. Indeed, in the model the measurement has been assumed to be instantaneous while in the experiment it is a dissipative process of a duration of about 1 μs. Furthermore, we can see in the figure, that for small values of $\mu^{(2)}$, that is in the Zeno regime, the two averages $\overline{\mathcal{P}}_g$ and $\overline{\mathcal{P}}_a$, playing the role of time and ensemble averages, practically coincide. This has been predicted by approximating the discrepancy between the two quantities as $\Delta q(\mu,\ m) \approx \frac{m^2}{2}(\Delta^2 H)^2(\nu_4 - \nu_2^2)$, which is of fourth order in $\mu^{(1)},\ \mu^{(2)}$. Note that figure 2 corresponds to two cases of the lower panel of figure 5.

4. Discussion and conclusion

We have analytically demonstrated the occurrence of an ergodic property when a quantum system is perturbed by an external environment that effectively measures the system at random times with its dynamics approaching a Zeno regime. In particular, we exploit large deviation theory to prove that the most probable value of the probability for the system to be in a given state equals to the non-stochastic case when the Zeno condition holds. Furthermore, we have experimentally tested these results along the transition to the Zeno regime using a BEC of Rubidium atoms which are trapped on an atom chip. Then, since the discrepancy between the statistical averages, here investigated, do strongly depend on the second and fourth statistical moments of the noise distribution $p(\mu)$ outside the Zeno regime, one could effectively determine the influence of the stochastic noise source on the dynamics of a fully controlled quantum system, hence characterising the external environment.

On top of that, although we have explicitly studied Hamiltonian dynamics and applied the projective measurement on an initial pure state, the method can be also generalised to arbitrary mixed input states with the dynamics being described by completely positive trace-preserving maps [30] and to the case of measurements projecting the system on higher dimensional Hilbert subspaces, hence leading to Stochastic Quantum Zeno Dynamics [25, 26, 32]. Finally, these results are expected to represent further steps towards controlled manipulations of quantum systems via dissipative interactions [33, 34] where one can indeed control the noisy environment or part of it in order to perform desired challenging tasks like the ones necessary for future quantum technologies.

Acknowledgements

We acknowledge fruitful discussions with S Ruffo, S Gupta, and A Smerzi. We thank M Schramböck (Atominstitut, TU-Wien) at the ZMNS (TU-Wien) who realised the atom chip we have used. This work was supported by the Seventh Framework Programme for Research of the European Commission, under the CIG grant QuantumBioTech, by the Italian Ministry of Education, University and Research (MIUR), under PRIN Grant No. 2010LLKJBX and FIRB Grant Agreements No. RBFR085XVZ and No. RBFR10M3SB, and by Ente Cassa di Risparmio di Firenze through the project Q-BIOSCAN.

Appendix A. Derivation of equation (12)

To derive equation (12) let us consider the series expansion of q^m and its logarithm up to fourth order, namely

$$q^m = 1 - m\Delta^2 H\mu^2 + \frac{m}{12}[\gamma_H + 3(2m-1)(\Delta^2 H)^2]\mu^4 + \mathcal{O}(\mu^6)$$

and

$$\ln q^m = -m\Delta^2 H\mu^2 + \frac{m}{12}[\gamma_H - 3(\Delta^2 H)^2]\mu^4 + \mathcal{O}(\mu^6),$$

where $\gamma_H \equiv \overline{H^4} - 4\overline{H^3}\,\overline{H} + 6\overline{H^2}\,\overline{H}^2 - 3\overline{H}^4$ is the kurtosis of the Hamiltonian. Hence, within this fourth order approximation $\Delta q(\mu, m)$ reads

$$\begin{aligned}\Delta q &\approx m\Delta^2 H\nu_2 - \frac{m}{12}[\gamma_H - 3(\Delta^2 H)^2]\nu_4 \\ &\quad + \ln\left\{1 - m\Delta^2 H\nu_2 + \frac{m}{12}[\gamma_H + 3(2m-1)(\Delta^2 H)^2]\nu_4\right\} \\ &\approx \frac{m^2}{2}(\Delta^2 H)^2\nu_4 - \frac{m^2}{2}(\Delta^2 H)^2\nu_2^2.\end{aligned}$$

Appendix B. Derivation of equation (13)

To derive equation (13) let us write the survival probability $\mathcal{P}(\{\mu_j\})$ as

$$\mathcal{P} = q(\mu^{(1)})^{k(\mathcal{P})} q(\mu^{(2)})^{m-k(\mathcal{P})},$$

and taking the logarithm of $\mathcal{P}$. Equation (14) then follows by resolving for $k(\mathcal{P})$. Moreover, the frequency $k(\mathcal{P})$ is binomially distributed, namely

$$\mathrm{Prob}(k(\mathcal{P})) = \frac{m!}{k(\mathcal{P})!(m-k(\mathcal{P}))!} p_1^{k(\mathcal{P})} p_2^{m-k(\mathcal{P})}.$$

Hence, by using the Stirling approximation, for m sufficiently large the binomial distribution $\mathrm{Prob}(k(\mathcal{P}))$ can be approximated by a Gaussian one, thus yielding equation (13).

References

[1] Gallavotti G 1995 *J. Stat. Phys.* **78** 1571
[2] von Neumann J 1929 *Z. Phys.* **57** 30
Tumulka R 2010 *Eur. Phys. J. H* **35** 201 (Engl. transl.)
[3] von Neumann J 1932 *Annals of Mathematics* **33** 587
[4] Wigner E 1932 *Phys. Rev.* **40** 749
[5] Peres A 1984 *Phys. Rev.* A **30** 504
[6] Goldstein S, Lebowitz J L, Tumulka R and Zanghì N 2010 *Eur. Phys. J.* H **35** 173
[7] Zhang D, Quan H T and Wu B 2016 *Phys. Rev.* E **94** 022150

[8] Asadi P, Bakhshinezhad F and Rezakhani A T 2016 *J. Phys. A: Math. Theor.* **49** 055301
[9] Neill C *et al* 2016 *Nat. Phys.* **12** 1037–41
[10] Hale J K 1988 *Asymptotic Behaviour of Dissipative Systems, Mathematical Surveys and Monographs n. 25* (Providence, R.I.: American Mathematical Society)
[11] Ellis R 2006 *Entropy, Large Deviations, and Statistical Mechanics* (New York: Springer)
[12] Touchette H 2009 *Phys. Rep.* **478** 1
[13] Dembo A and Zeitouni O 2010 *Large Deviations Techniques and Applications* (Berlin: Springer)
[14] Gallavotti G, Lebowitz J L and Mastropietro V 2002 *J. Stat. Phys.* **108** 831
[15] Netočný K and Redig F 2004 *J. Stat. Phys.* **117** 521
[16] Garrahan J P and Lesanovsky I 2010 *Phys. Rev. Lett.* **104** 160601
[17] Lesanovsky I, van Horssen M, Guţă M and Garrahan J P 2013 *Phys. Rev. Lett.* **110** 150401
[18] Breuer H P and Petruccione F 2003 *The Theory of Open Quantum Systems* (Oxford: Oxford University Press)
[19] Misra B and Sudarshan E C G 1977 *J. Math. Phys.* **18** 756
[20] Facchi P and Pascazio S 2002 *Phys. Rev. Lett.* **89** 080401
[21] Smerzi A 2012 *Phys. Rev. Lett.* **109** 150410
[22] Itano W M, Heinzen D J, Bollinger J J and Wineland D J 1990 *Phys. Rev.* A **41** 2295
[23] Kwiat P, Weinfurter H, Herzog T, Zeilinger A and Kasevich M A 1995 *Phys. Rev. Lett.* **74** 4763
[24] Fischer M C, Gutierrez-Medina B and Raizen M G 2001 *Phys. Rev. Lett.* **87** 040402
[25] Shushin A I 2011 *J. Phys. A: Math. Theor.* **44** 055303
[26] Gherardini S, Gupta S, Cataliotti F S, Smerzi A, Caruso F and Ruffo S 2016 *New J. Phys.* **18** 013048
[27] Müller M M, Gherardini S, Smerzi A and Caruso F 2016 *Phys. Rev.* A **94** 042322
[28] Schäfer F, Herrera I, Cherukattil S, Lovecchio C, Cataliotti F S, Caruso F and Smerzi A 2014 *Nat. Comm.* **5** 4194
[29] Given the initial state $|\psi_0\rangle$, we define the expectation value of the $k-th$ power of the system Hamiltonian H as $\langle H^k\rangle \equiv \langle\psi_0|H^k|\psi_0\rangle$, $k = 0,\ 1,\ldots$, and $\Delta^2 H \equiv \langle H^2\rangle - \langle H\rangle^2$ as the variance of the energy.
[30] Caruso F, Giovannetti V, Lupo C and Mancini S 2014 *Rev. Mod. Phys.* **86** 1203
[31] Lovecchio C, Schäfer F, Cherukattil S, Khan M A, Herrera I, Cataliotti F S, Calarco T, Montangero S and Caruso F 2016 *Phys. Rev.* A **93** 010304(R)
[32] Müller M M, Gherardini S and Caruso F 2016 arXiv:1607.08871
[33] Turchette Q A, Myatt C J, King B E, Sackett C A, Kielpinski D, Itano W M, Monroe C and Wineland D J 2000 *Phys. Rev.* A **62** 053807
[34] Schindler P, Müller M, Nigg D, Barreiro J T, Martinez E A, Hennrich M, Monz T, Diehl S, Zoller P and Blatt R 2013 *Nat. Phys.* **9** 361